

Evaluation for Risk of Cascading Failures in Power Grids by Inverse-Community Structure

Xiaoliang Wang, Fei Xue, Qigang Wu, Shaofeng Lu, Lin Jiang and Yue Hu

Abstract—Recently, the development of the Internet of Things (IoT) enables more comprehensive and intelligent analysis and defense for cascading failures in power grids. This paper summarizes power grids as Temporal Weighted Networks (TWN) which are different from conventional temporal networks. For TWN, the topological structure is fixed but weight distribution is time-varying. Then it is noted that for different operating states represented by different weight (power flow) distribution at different time sections, the risks of cascading failures would be completely different. Inspired by analysis of inter-subnetworks power shifts in cascading failures, Inverse-Community (IC) structure is proposed in TWN to intuitively identify the risk of cascading failures. IC describes a structure in weighted networks with several communities in which the weighted interaction between communities is significantly stronger than that within the same community. Furthermore, the conventional modularity is upgraded as Inverse Modularity (IM) to quantify the characteristic of IC structure in power networks. Subsequently, considers the risk of cascading failures represented by IM and the cost of power network operation, a security/economic dispatch (SED) method is designed to handle the optimal power dispatch issues. Simulation results prove a positive correlation between IM of power flow distribution and risk of cascading failures. Furthermore, the results on the IEEE 118-bus system demonstrate the effectiveness of the proposed SED method in mitigating cascading failure risks.

Index Terms— Inverse-community structure, temporal weighted network, cascading failure, security/economic dispatch, Internet of Things (IoT), complex network.

I. INTRODUCTION

With the rapid growth of demand and scale of topology in power networks, the power outages caused by cascading failures have catastrophic consequences to the stability and reliability of power grids, which will have severe impacts on public life and economic cost for society [1-3]. The process of cascading failure contains multifarious causes, such as the topological feature, loading level of transmission lines, power flow distribution, fault components and external factors.

Modern power systems have been widely recognized as typical Internet of Things (IoT) systems with more cyber technologies and devices involved. IoT is a supplement to

power grids, has developed rapidly [4]. As typical Cyber-Physical System, most studies about security of modern power systems from IoT perspective mainly focus on cyber security issues [5-7]. However, the vulnerability of physical components to cascading failures could be utilized or amplified by IoT measures and background. Cascading failures propose a major challenge to the reliability of IoT systems [8], [9]. Up to now, a great diversity of strategies has been proposed to analyze cascading failures in power systems; these approaches capture different mechanisms during the cascading failures. Due to uncertainties and unforeseeable factors that could cause cascading, the researchers propose stochastic simulation approaches to simulate more possible events. For example, a Markov chain is a stochastic process that is adopted to modeling the stochastic factors in cascading failures of a power network [10]. In [11], a stochastic Markov chain model based on power flow redistribution is presented to capture the cascading events, which considers the load setting, generation and line flow.

In addition, high-level statistical models can describe the cascading process but ignore some specific mechanisms in the cascading failure process, such as the power grid structures, the interactions of power system components [12]. Such models are tractable and straightforward, which reduces the simulation time. For example, the CASCADE model in [13] is based on load of components, where some components may fail because load exceeds a certain threshold, which will redistribute the load of other components, thus forming a cascading. Meanwhile, several researchers analyze cascading failures from the perspective of complex network theory. For instance, the study in Ref. [14] considers a topological perspective in which the effective graph resistance is proposed to relate the topology of a power grid to its robustness against cascading failures. Some studies consider the propagation probability among each bus's outage and generate a graph to describe the possible cascading failure propagation path [15], [16]. Ref. [17] analyzed the critical buses in a network from the aspect of network robustness.

The aforementioned cascading failure analysis methodologies have their own advantages and disadvantages. The stochastic simulation approaches consider all possible uncertainties but fail to simulate the dynamics of the power

This work was supported in part by the Research Development Fund (RDF-15-02-14 and RDF-18-01-04) of Xi'an Jiaotong-Liverpool University, and in part by the National Natural Science Foundation of China (51877181).

X. Wang, F. Xue and Q. Wu are with the Department of Electrical and Electronic Engineering, Xi'an Jiaotong-Liverpool University, Suzhou 215123, Jiangsu, China. X. Wang and Q. Wu are also with the University of Liverpool, Liverpool, U.K. (email: Fei.Xue@xjtu.edu.cn).

S. Lu is with the Shien-Ming Wu School of Intelligent Engineering,

Guangzhou International Campus, South China University of Technology. (email: lushaofeng@scut.edu.cn).

L. Jiang is with the Department of Electrical Engineering and Electronics, The University of Liverpool, Liverpool, L69 3GJ, U.K. (email: l.jiang@liverpool.ac.uk).

Y. Hu is with Shanghai Jiao Tong University, Shanghai 200240, China (email: yuehu@sjtu.edu.cn).

system [10]. High-level statistical models neglect some detailed mechanisms of cascading failure to simulate the propagation of cascading failure quickly. The complex network methods can investigate the robustness, critical components, and structure of a power network, but they are still based on the static structural characteristics of power grids. However, the temporal features of operation status also have a significant impact on cascading failure process, which are commonly neglected in current complex network approaches.

Moreover, as power networks thrive in recent decades, there emerges an essential issue to ensure economic operation under the premise of security of power systems. The conventional method is to set security constraints for economic dispatch, which is known as security constrained economic dispatch (SCED) [18-21]. SCED ensures the safe operation of power network by setting different constraints such as power balance, preventing overloading of transmission lines, the output limits of generators and renewable energy sources, and so on. Besides economic costs, other factors could be integrated in power dispatch as a multi-objective optimization problem, such as environmental/economic dispatch (EED) [22-24]. However, almost no existing power dispatch methods consider the risk of cascading failures as one of the objectives. The existing cascading failure analysis methodologies are mainly based on complicated simulations. Meanwhile, the large numbers of possible $N-k$ combinations make large-scale power system outage assessment computationally prohibitive [25]. So, it is difficult for most existing studies on optimal power dispatch to involve the risk of cascading failures in objective functions.

Corresponding to the abovementioned defects in cascading failure analysis and power dispatch, this paper makes contributions in following three points:

- First, **Inverse-Community (IC)** is defined as the structure with several communities (subnetworks) in which the transmission of physical elements between communities is significantly stronger than interaction within the same community. This is to capture the key characteristics of operating states leading to cascading failures. Then, the conventional modularity [26] in detection of conventional communities is upgraded as **Inverse-Modularity (IM)** to quantify the extent of IC structures.
- Second, by simulation and comparison, a positive correlation between IM of power flow distribution and risk of cascading failures is justified.
- Third, an optimal power dispatch method called the **security/economic dispatch (SED)** that takes both the magnitude of IM, representing cascading failure risk, and the generation cost as objectives is proposed. The simulation results on the IEEE 118-bus system demonstrate that this approach can mitigate the threats of cascading failures while maintaining the cost economy.

The rest of the paper is organized as follows. Section 0 defines and discusses the concept of IC structure. Meanwhile, IM is defined, and the Newman fast algorithm is redesigned to detect IC structures. Section III provides the security/economic dispatch method. Case studies and simulation results are discussed in Section IV.

II. FRAMEWORK OF INVERSE-COMMUNITY

A. Inverse-community structure in power flow distribution

Cascading failures are due to random initial contingencies

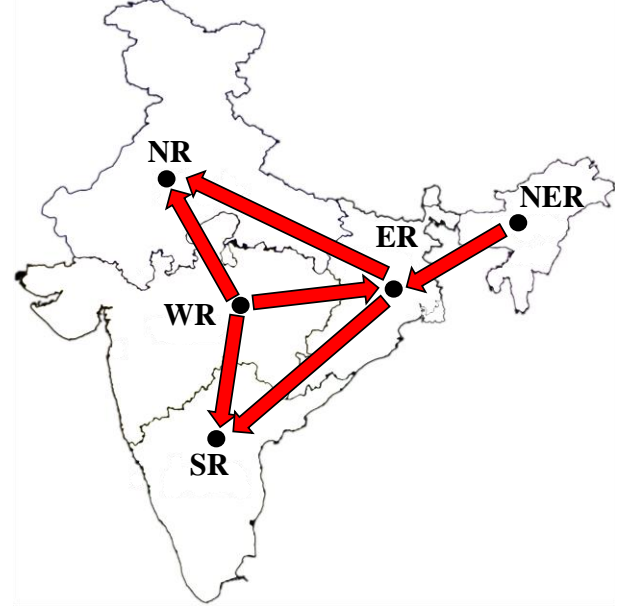


Fig. 1. The power exchange in 5 regions of India power grids before power blackouts.

such as transmission line outages, load variances, and system operators' mistakes. The propagation of the cascading failure can lead to large blackouts in a power network [10]. There are several cascading failures for the large-scale blackouts in the world in recent years. The 2012 two India blackouts caused substantial economic losses and social impacts [27]. The India power grid is demarcated into 5 regional grids which are Northern regions (NR), Eastern regions (ER), Western regions (WR), North Eastern regions (NER), and Southern regions (SR), in which NR, ER, NER, and WR are synchronously interconnected. SR is asynchronously connected to ER and WR. The sketch of the power exchange in 5 regions before the power blackouts is shown in Fig. 1. A large number of lines were out of service caused by system maintenance, line failure, voltage control and other factors near WR-NR interface before the first outage, which severely weakened their interconnections. There were only two lines between NR and WR to maintain the power grids operation. Further, before the accident, WR exported large scale power to NR through the 400 KV Bina-Gwalior line, which was under heavy load operation. At the beginning of the outage, due to the heavy load, the Bina-Gwalior line was tripped by distance protection. Then, the NR and WR power grids were disconnected. The power flows from WR to NR were transferred through ER, which aggravated the power flow in the transmission section and caused a big power swing in NR-ER interface which eventually led to cascading failures. The characteristics of this cascading failure process could be summarized as:

1. There are significant unbalance between power supply and load demand in local subnetworks. So large scale power shifts are performed between specific subnetworks.

2. Line connections between subnetwork boundaries are weak and sparse, but power transmission magnitudes on these lines are much stronger than internal lines.

3. Initial contingencies in boundary lines may cause power flow shifts to other relevant boundary lines which already have high loading level. Then cascading failures triggered by these lines become highly possible.

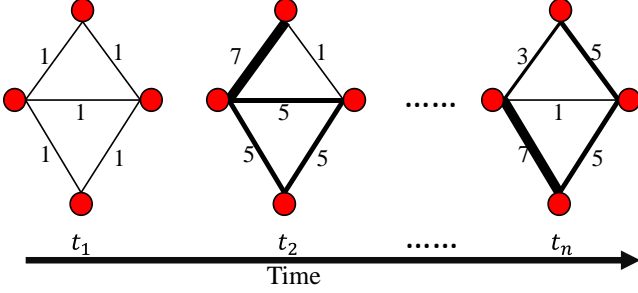


Fig. 2. An example to represent TWN.

In reference [28], the major cause of power grid cascading failure was identified as inter-subnetwork power shifts. A partitioning algorithm is developed to detect the subnetwork with excess or scarcity of generation, which are bridged by overloaded lines. The study in [28] just quantified the criticality of branches; it, nevertheless, did not propose a clear quantitative method for the overall evaluation of this inter-subnetwork power shifts. Furthermore, it did not verify the correlation between inter-subnetwork power shifts and cascading failure risks.

It is clear that even the topological connections in power grids are unchanging, different power flow distribution in all lines may be time-varying and cause different risks of cascading failures. In some existing studies, researchers investigate some dynamic systems using temporal network models, where edges connections may vary in time [29, 30]. However, in the targeted study time frame, the edges connections in power grids are fixed. Therefore, in this work, to describe the correlation between topological structure and operation status, power grids are summarized as **Temporal Weighted Networks (TWN)** which have fixed topological structure but time-varying weight distribution. Fig. 2 is an example to illustrate the TWN.

Inspired by the characteristics of cascading failures abovementioned, we propose the concept of **Inverse-Community (IC)** in TWN that could be defined as a weighted network structure with communities in which the weights of boundary lines between communities are much larger than lines inside communities. From physical perspective, this represents that inter-community interactions (such as power transmission) are much stronger than internal interactions. In TWN, the weights of lines may vary with time, IC is to capture the weight distribution feature for a specific time section. IC in power flow distribution could embody the effect of inter-subnetwork power shifts abovementioned as cause of cascading failures.

Fig. 3 is the sketch of networks with inverse-community and normal community structures. The most obvious difference between these two network structures is reflected in the weight distribution. The larger weight is distributed on boundary lines between the communities in IC structure, which is the opposite of normal communities. The feature of IC can be summarized as

- Topological connection is consistent with conventional meaning of community: more density of internal connections and low density of external connections;
- Weight of external connection is much higher than

internal connection;

- The stronger the characteristics of IC, the higher risks of cascading failures.

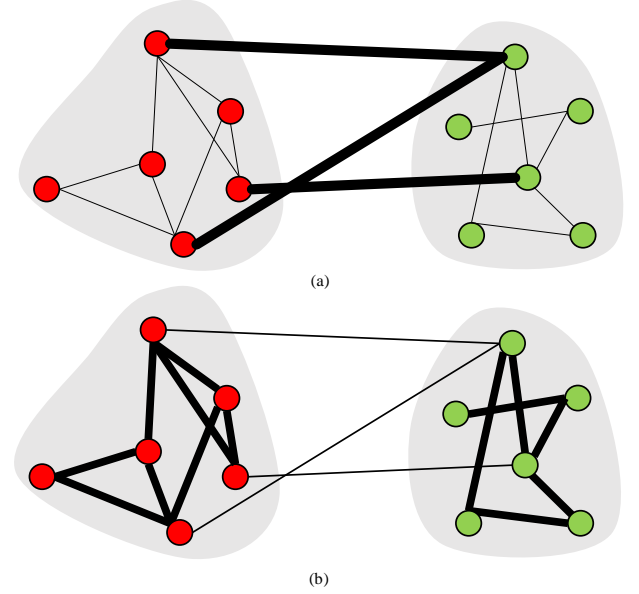


Fig. 3. The example of (a) inverse community and (b) normal community. The network is constituted of two communities which are connected by some critical branches. (The thickness of the branch indicates the magnitude of the weight).

B. Inverse modularity of power flow distribution

In conventional community detection, modularity Q [26, 31, 32] is an index to quantitatively evaluate partitioning results and is extensively handled to investigate the community structure in networks [33-37]. To be specific, the higher the value of Q , the better the partitioning [38]. Modularity Q can be regarded as the difference between the proportion of edges connected to the internal nodes of a community and the expected value of that proportion in a random network, which is calculated as

$$Q = \sum_{ij} \left[\frac{A_{ij}}{2m} - \frac{k_i}{2m} \frac{k_j}{2m} \right] \delta(g_i, g_j), \quad (1)$$

where A_{ij} that can be expressed as (2), is the element in the adjacency matrix \mathbf{A} . m is equal to $\frac{1}{2} \sum_{ij} A_{ij}$ which denotes the number of branches in the network. k_i is the number of edges connected to a node i . $g_i(g_j)$ is the community that node $i(j)$ belongs to. The δ -function $\delta(g_i, g_j)$ equals to 1 if nodes i and j are in the same community and 0 otherwise.

$$A_{ij} = \begin{cases} 1, & \text{if there is a branch joining nodes } i \text{ and } j, \\ 0, & \text{otherwise.} \end{cases} \quad (2)$$

As aforementioned, IC can indicate more transmission of physical elements (such as power flow) between community boundaries than within the communities. To quantify the IC extent in weight distribution of TWN, the conventional modularity is then upgraded.

First, we propose a temporal weight ω_{vw} that considers the structural characteristic and operating conditions of power grids to quantify the power flow distribution of a certain time section. The temporal weight ω_{vw} is defined as

$$\omega_{vw} = \frac{1}{|P_f^{vw}|}, \quad (3)$$

where $|P_f^{vw}|$ is the absolute value of power flow of branch l_{vw} from bus v to bus w , which describes the operating conditions of power grids at a particular moment. **The smaller value of ω_{vw} denotes that the branch sustains larger power transfers.**

Considering the structural characteristics of power networks, a temporal weight matrix ω_{vw} is defined as

$$\omega_{vw} = \begin{cases} \omega_{vw}, & \text{if bus } v \text{ and } w \text{ are connected,} \\ 0, & \text{otherwise.} \end{cases} \quad (4)$$

Then, similar to conventional modularity, the concept of **inverse-modularity** Q_{inv} is defined by temporal weight to quantify the extent of IC. The Q_{inv} can be calculated by

$$Q_{inv} = \sum_{vw} \left[\frac{\omega_{vw}}{2W} - \frac{\omega_v}{2W} \frac{\omega_w}{2W} \right] \delta(c_v, c_w), \quad (5)$$

where ω_{vw} is the corresponding element in the temporal weight matrix ω . W is the total temporal weight of whole power grids, which can be computed as (6). ω_v (ω_w) is the temporal weight degree of bus v (w) that is calculated as (7).

$$W = \frac{1}{2} \sum_{vw} \omega_{vw}. \quad (6)$$

$$\omega_v = \sum_w \omega_{vw}, \quad \omega_w = \sum_v \omega_{vw}. \quad (7)$$

To make the physical meaning of modularity clear to readers, a virtual scenario could be considered to make following explanation. In a known power network (**PN**), fictitiously, if one unit of temporal weight is taken randomly, the probability of this unit of temporal weight connecting from node v to node w should depend on two events: (1) Event 1: this unit of temporal weight is connected to node v ; (2) Event 2: this unit of temporal weight is connected to node w .

The probability of Event 1 is equal to $\omega_v/2W$. For **PN**, the value of temporal weight among node v and node w is already known. Event 1 and 2 are not independent. Therefore, the probability of Event 2 is ω_{vw}/ω_v , which means that the probability of this unit of temporal weight between node v and node w can be computed as

$$B_{vw} = \frac{\omega_v}{2W} \cdot \frac{\omega_{vw}}{\omega_v} = \frac{\omega_{vw}}{2W}. \quad (8)$$

Then, a benchmark network (**RN**) is designed with the same number of nodes and the total value of temporal weight as **PN**. The distribution of temporal weight is random in **RN**, but the temporal weight degree of any node is equal to that in **PN**. Consequently, events 1 and 2 are independent in **RN**, that is, the probability corresponding to Event 1 and Event 2 are respectively equivalent to $\omega_v/2W$ and $\omega_w/2W$ when one unit of temporal weight is randomly selected from **RN**. Hence, the probability of this unit of temporal weight connecting node v and node w in **RN** is equal to

$$P_{vw} = \frac{\omega_v}{2W} \cdot \frac{\omega_w}{2W}. \quad (9)$$

Here, IM Q_{inv} in (5) is the probability difference of one unit of temporal weight connecting node v and w between **PN** and the benchmark **RN**.

C. Detection of inverse-community

By defining temporal weight as reciprocal of power flow, the detection of IC has been simply converted to detection of normal communities. For example, the IC of power flow distribution in (a) of Fig. 3 is equivalent to normal community of temporal weight in (b). Then the classical Newman fast algorithm [26] for weighted networks can be applied by replacing the modularity with IM. The IC detection algorithm is outlined in **Algorithm 1**.

| Algorithm 1: Inverse-community detection for power supply network partitioning | |
|---|--|
| Input: | network data, temporal weight matrix |
| Output: | partitioned result |
| 1: | Initialize power network with N communities; |
| 2: | Calculate the inverse modularity Q_{inv} ; |
| 3: | while the number of communities is not 1 do |
| 4: | Calculate the increments of inverse modularity ΔQ_{inv} ; |
| 5: | Select the partitioning with maximum ΔQ_{inv} |
| 6: | Recalculate Q_{inv} according to the result of partitioning; |
| 7: | Conserve the number of communities (The maximum number of mergers is N-1); |
| 8: | end while |

III. SECURITY/ECONOMIC DISPATCH

Considering the catastrophic consequences to the stability and reliability of power grids caused by cascading failures, we propose the **security/economic dispatch (SED)** method to reduce the severity of cascading failure and minimize the generation cost. It should be noted that the proposed power dispatch approach is not always required on all time sections, that is, SED is only performed when IM corresponding to the power flow distribution is greater than a critical value, which indicates high risk of cascading failure. The specific process is as follows:

Step 1: Obtain the power dispatch based on conventional OPF;
Step 2: Calculate the corresponding inverse-modularity Q_{inv} ;
Step 3: Determine whether Q_{inv} is larger than $Q_{critical}$;
Step 4: If Q_{inv} is larger than $Q_{critical}$, perform the SED. Otherwise, retain the power dispatch results obtained by OPF.

As discussed in Section 0, the stronger the IC feature, the greater the risk of cascading failures. IM is presented to quantify the extent of IC; namely, the big magnitude of IM represents the network state with a stronger IC feature, signifying that this network has a higher risk of cascading failure. In other words, we can apply IM to quality the impact of cascading failure or the network vulnerability, which means the lower the IM, the higher the security of system operation. Hence, in this work, the SED method minimizes simultaneously two objective functions, IM and the cost. The following paragraph formulated two objectives and several constraints.

A. Objectives

1) *Minimization of IM:* The security objective is to minimize the magnitude of the IM Q_{inv} for current network state, and it can be expressed as

$$Q_{inv}(P_G) = \text{Min} \left[\sum_{vw} \left[\frac{\omega_{vw}}{2W} - \frac{\omega_v}{2W} \frac{\omega_w}{2W} \right] \delta(c_v, c_w) \right]. \quad (10)$$

2) *Minimization of Generation Cost:* The objective of economics is to minimize cost. The minimization of total

generation cost is computed by quadratic cost curve [39], which can be represented as

$$F(P_G) = \text{Min} \left[\sum_{i=1}^{N_G} a_i + b_i P_{G_i} + c_i P_{G_i}^2 \right], \quad (11)$$

where N_G is the total number of generators; a_i , b_i and c_i are the cost coefficients of the i th generator; P_{G_i} is the real power output corresponding to the i th generator.

The real power output of generators P_G is the vector of decision variables, which presents as follows

$$P_G = [P_{G_1}, P_{G_2}, \dots, P_{G_{N_G}}]^T. \quad (12)$$

B. Constraints

1) *Generation Capacity Constraint*: The active power of each generation should be restricted by lower and upper limits as

$$P_{G_i}^{\min} \leq P_G \leq P_{G_i}^{\max}, i = 1, 2, \dots, N_G, \quad (13)$$

where $P_{G_i}^{\min}$ and $P_{G_i}^{\max}$ are the minimum and maximum output power on generation bus i ; N_G is the total number of generators.

2) *Power balance constraint*: The total power outputs of generators must satisfy the demand of loads P_D . Therefore

$$\sum_{i=1}^{N_G} P_{G_i} - P_D = 0. \quad (14)$$

3) *Power flow constraint*: For the secure operation of the network, the transmission line loading S_{l_k} should be within its upper limit as

$$S_{l_k} \leq S_{l_k}^{\max}, k = 1, 2, \dots, N_L, \quad (15)$$

where $S_{l_k}^{\max}$ is the maximum power flow limitation on transmission line k ; N_L is the total number of transmission lines.

C. Formulation

The **SED** problem can be mathematically formulated as a nonlinear multi-objective optimization problem through combining the objectives and constraints, which is described as follows.

$$\text{Minimize } F(P_G), Q_{inv}(P_G) \quad (16)$$

Subjected to

$$\begin{aligned} \sum_{i=1}^{N_G} P_{G_i} - P_D &= 0 \\ P_{G_i}^{\min} &\leq P_G \leq P_{G_i}^{\max}, i = 1, 2, \dots, N_G \\ S_{l_k} &\leq S_{l_k}^{\max}, k = 1, 2, \dots, N_L. \end{aligned} \quad (17)$$

D. Security/economic dispatch method

In this paper, the conventional genetic algorithm (GA) is applied to find the Pareto-optimal set (or Pareto-optimal front) in **SED** problem. The fitness function computes the multi-objective function in (16). To ensure the feasibility of Pareto-optimal solutions, the population and generation in GA should be constrained by (17) in the feasible region. The GA is utilized to generate a new population until the maximum value of generation is reached.

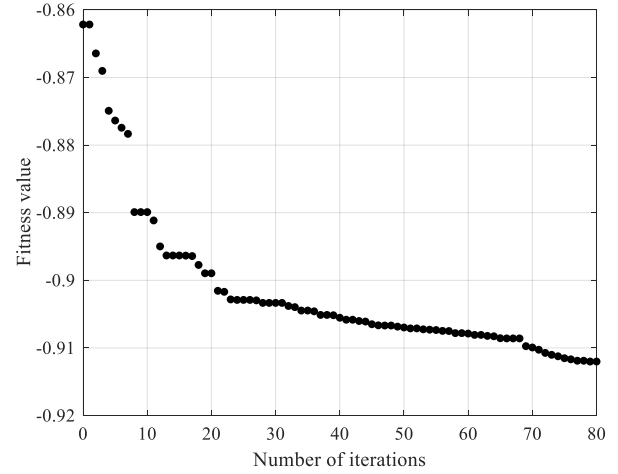


Fig. 4. The fitness objective value of different iterations in IEEE 118-bus system in searching maximum IM.

IV. CASE STUDY

A. *The correlation between inverse-community structure and risk of cascading failures.*

To find power dispatch solutions with different levels of IM, a genetic algorithm is designed to search for a state in which the generators outputs make the largest inverse-modularity for given load conditions. The objective function is set as the maximum inverse modularity Q_{inv} :

$$\begin{aligned} f(P_G) &= \text{Max } Q_{inv}(P_G) \\ &= \text{Max} \left[\sum_{vw} B_{vw} - P_{vw} \delta(c_v, c_w) \right]. \end{aligned} \quad (18)$$

To verify the severity of the cascading failures, MATCASC [40] that is a tool based on MATPOWER is used to simulate cascading failure process. Some studies [41-43] in recent years have applied this tool to successfully simulate cascading failures. MATCASC can capture the line overloads and islanding effect by deploying a DC load flow analysis. The power network may disintegrate into some islands due to the removal overloaded lines. The MATCASC will check the islands at each cascading stage and redistribute the electrical power. This tool estimates power flows across the power grid and models line protections. A line will be deenergized by the protection mechanism when the line exceeds the load threshold. Meanwhile, this software package provides different line threat determination modules, including three removal strategies, such as random removal, edge betweenness centrality and electrical node significance, to trigger the cascading failure in power grids [40]. MATCASC assumes that the maximum capacity of a branch is calculated by the product of tolerance parameter α_i and initial load. Considering the real engineering features of power networks, we set the maximum capacity of branch to a fixed value according to the actual data of network. Besides, this paper proposes another removal strategy based on the power flow rank of boundaries of IC to initiate cascading failures.

Fig. 4 shows that the value of the most fitness objective continues decreasing and finally it converges at 0.912 in the IEEE 118-bus system. From this converging process, we chose some other power dispatching scenarios with different level of IM in power flow distribution. Then with simulations by MATCASC, cascading failures in each scenario are triggered

by removing most loaded boundary lines, and their value of remaining loads after cascading failures are calculated. Fig. 5 presents the IM corresponding to different power dispatching scenarios and remaining loads after cascading failures in IEEE-118 and IEEE-300 bus systems. It can be obviously found that as the value of IM Q_{inv} increases, the value of remaining loads in network decrease. Therefore, the stronger the IC characteristics of the network, the more serious the loss caused by cascading failures in the network. **This can prove that the inverse-modularity has a positive correlation with risk of cascading failures.**

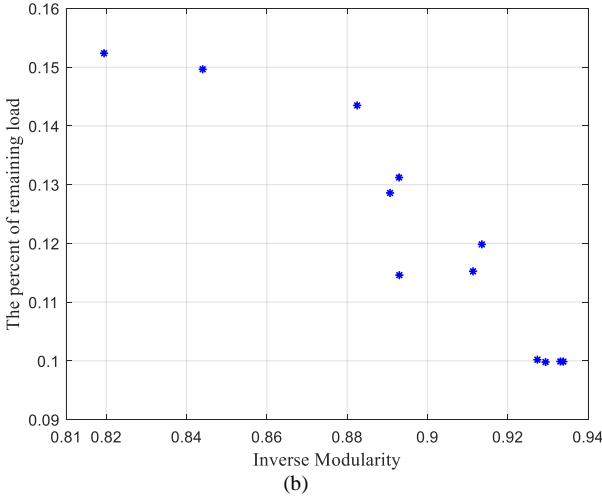
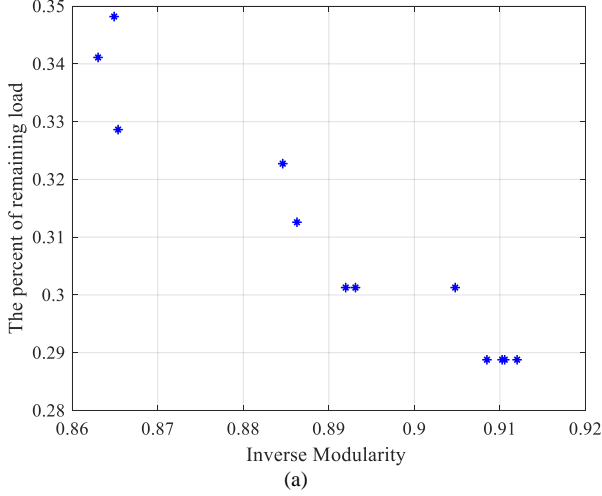


Fig. 5. The IM and remaining load corresponding to different power dispatching schemes in (a) IEEE 118-bus system, (b) IEEE-300 bus system.

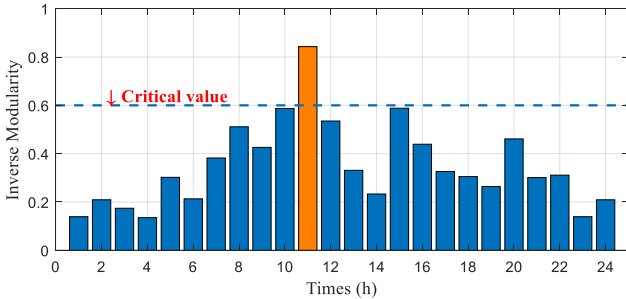


Fig. 6. The IM per hour for different loads condition.

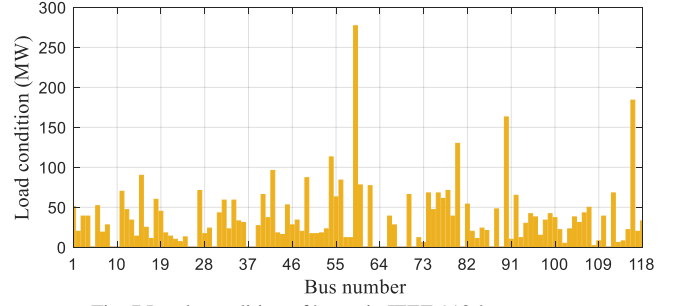


Fig. 7 Loads condition of buses in IEEE 118-bus system.

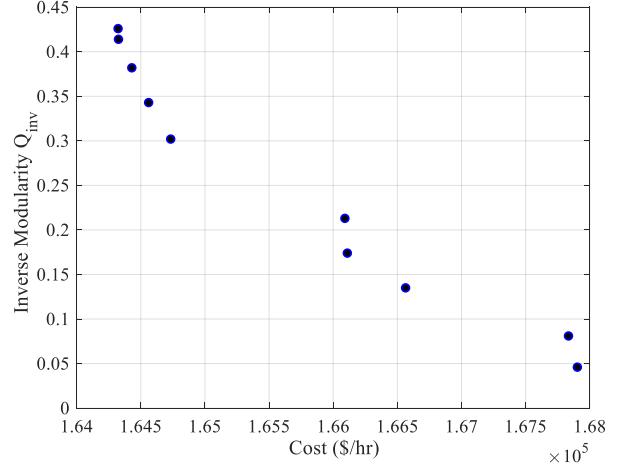


Fig. 8. Pareto front obtained by SED method for IEEE 118-bus system.

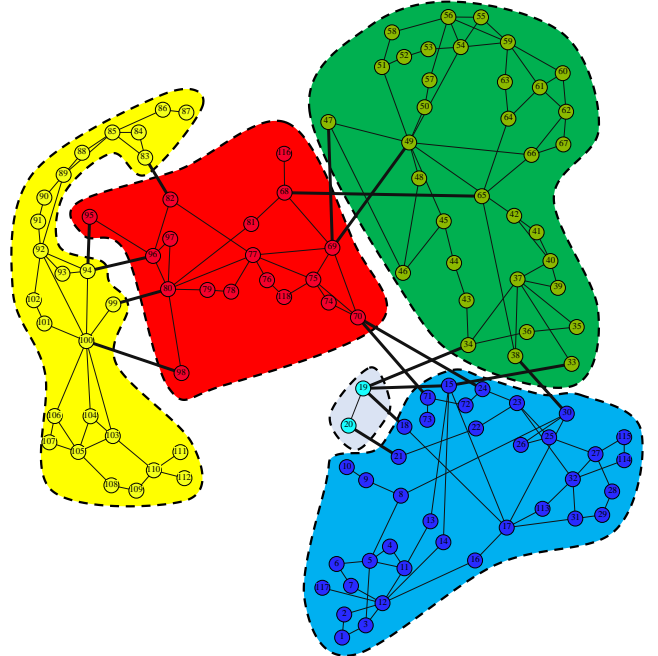


Fig. 9. The partitioning results of inverse community for solution S_5 .

B. SED on the IEEE 118-bus system

In this paper, the IEEE 118-bus system is applied as a test case to analyze and assess the performance of the proposed SED method. All the computations were performed in MATLAB. In the process of simulation, the population size was fixed at 200. The size of Pareto-optimal set was set as 10. Meanwhile, the crossover and mutation ratios were respectively chosen as 0.8 and 0.01.

At first, different load conditions in 24 hours are randomly

modeled and power dispatch per hour is performed by conventional OPF which only minimizes generation cost. Fig. illustrates the IM corresponding to each hour. The critical value of IM is set as $Q_{critical} = 0.6$. The IM of the bar with orange color is larger than $Q_{critical}$. Then, this case of power dispatch by conventional OPF is considered as **Case 1**. The generation cost of Case 1 is 125948 \$/hr. The load condition of case 1 is presented in Fig. . Then the proposed SED method is applied on Case 1, and the Pareto front of SED method is shown in Fig. . Furthermore, Table I presents the magnitude of IM and cost, corresponding to each solution at Pareto front. Then, MATCASC is used to simulate the cascading failures in different cases. To further explain the proposed removal strategy, the solution S_5 is chosen as an example.

Table I The inverse modularity and cost of each solution at Pareto front.

| SED solutions | Inverse modularity Q_{inv} | Cost (\$/hr) |
|---------------|------------------------------|---------------|
| S_1 | 0.426 | 164323 |
| S_2 | 0.414 | 164326 |
| S_3 | 0.382 | 164430 |
| S_4 | 0.343 | 164561 |
| S_5 | 0.302 | 164733 |
| S_6 | 0.213 | 166091 |
| S_7 | 0.174 | 166110 |
| S_8 | 0.135 | 166564 |
| S_9 | 0.081 | 167834 |
| S_{10} | 0.046 | 167903 |

Table II. The power flow of inverse community boundaries in solution S_5 .

| From bus | To bus | Power flow(MW) | From bus | To bus | Power flow(MW) |
|----------|--------|----------------|----------|--------|----------------|
| 30 | 38 | 176.7 | 15 | 33 | 43.9 |
| 70 | 71 | 124.2 | 82 | 83 | 41.1 |
| 65 | 68 | 88.7 | 19 | 34 | 37.0 |
| 94 | 95 | 62.3 | 47 | 69 | 31.4 |
| 98 | 100 | 50.1 | 18 | 19 | 29.3 |
| 80 | 99 | 45.6 | 49 | 69 | 27.8 |
| 24 | 70 | 44.8 | 15 | 19 | 19.0 |

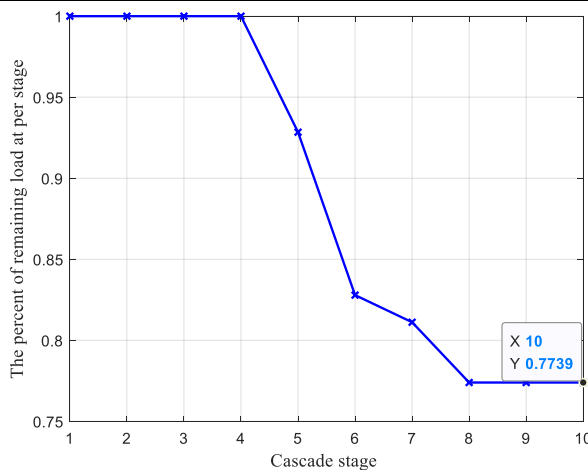


Fig. 10. The percent of remaining load at per stage of cascade for solution S_5 .

Fig. 9 presents the partitioning results of IC for solution S_5 , in which the different colours are utilized to represent diverse ICs. Meanwhile, the bold lines represent the boundaries between each IC. Table II shows the rank of boundaries power flow of solution S_5 . Fig. is the simulation results on the severity of the cascading failure of S_5 when two boundary lines (30-28 and 70-71) are attacked according to the power flow rank of IC boundary lines, which suggests that the remaining load is almost 77%. In Addition, the initial failure propagates into the network very slowly, that is, this SED method provides a larger

tolerance capability that can supply more time to the network operator to take preventive actions to better handle the cascading failure. As discussed in Section III, it is not necessary to use SED for all operation status. For example, the critical value for IM is set as 0.6. The proposed power dispatch approach should be performed only when the IM is larger than $Q_{critical}$ (0.6) to reduce the cost and time.

Furthermore, in Fig. 10, power supply could be maintained in case of one line disconnected. However, after more lines broken, cascading failure could be triggered. Even a power dispatch solution follows N-1 principle, it could be still vulnerable from N-k perspective. However, as indicated in other previous studies, simulation-based evaluation of N-k contingencies would be very time-consuming. But in this paper, this vulnerability is expected to be captured and quantitatively assessed directly by IC and IM without exhausting screening for all possible N-k contingencies.

C. Comparison against conventional OPF

This section compares the SED method with the conventional OPF based on MATPOWER to in-depth investigate the proposed method. The conventional OPF

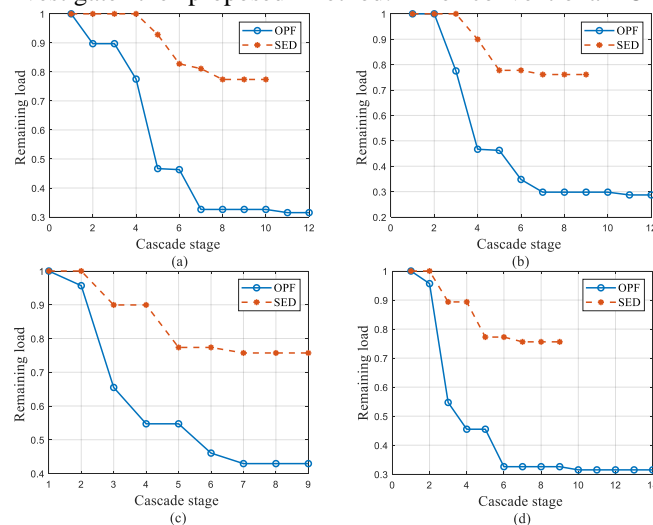


Fig. 5. The severity of the cascading failures triggered by attacking different numbers of boundary lines: (a) 2 lines (b) 4 lines (c) 6 lines (d) 8 lines.

Table III. Comparison between Case 1 and different SED solutions.

| Q_{inv} | The percent of remaining load | | | | |
|-----------|-------------------------------|-----------------------|-----------------------|-----------------------|-------|
| | Attacked 2 boundaries | Attacked 4 boundaries | Attacked 6 boundaries | Attacked 8 boundaries | |
| Case1 | 0.843 | 31.5% | 28.7% | 42.9% | 31.5% |
| S_5 | 0.302 | 77.4% | 76.1% | 75.7% | 75.6% |
| S_6 | 0.213 | 78.9% | 78.9% | 79.8% | 78.0% |
| S_7 | 0.174 | 71.8% | 77.4% | 77.4% | 74.7% |
| S_8 | 0.135 | 77.4% | 76.1% | 75.6% | 75.6% |

regards only the generation cost as the objective function, which does not consider the cascading failure's risk. As abovementioned, the IM Q_{inv} of Case 1 dispatched by conventional OPF is 0.843 that is significantly higher than the SED solutions in Table II, which means that Case 1 has strong IC characteristic, that is, the impact of cascading failure is more serious. To verify this standpoint, we chose the power flow rank of IC boundary lines to initiate the cascading failures and compare Case 1 with the power dispatch solution obtained by the SED method. Fig. 5 depicts the severity of the cascading

failures triggered by attacking different numbers of boundary lines, which compares the results by Case 1 and the SED solutions S_5 . The results indicate that the remaining load of solutions S_5 is significantly higher than Case 1, which prove that the risk of the cascading failure in Case 1 is much higher than that of SED. Additionally, Table III compares the severity of the cascading failures in Case 1 and different SED solutions. The number of remaining loads of SED solutions are obviously higher than Case 1, which indicates that SED can effectively reduce the risk of cascading failures when settling multi-objective optimal power dispatch problem.

Table IV. The remaining load removal in Case 1 and different SED solutions.

| | The percent of remaining load | | |
|-------|-------------------------------|------------------------|------------------------------|
| | Random removal | Betweenness Centrality | Electrical Node Significance |
| Case1 | 25.1% | 32.5% | 32.5% |
| S_5 | 76.6% | 76.3% | 76.6% |
| S_6 | 76.6% | 76.2% | 76.6% |
| S_7 | 76.6% | 76.2% | 76.6% |
| S_8 | 79.5% | 76.2% | 76.6% |

Furthermore, according to the three removal strategies in [40], the corresponding cascading failures for Case 1 and SED solutions are also simulated. The results are shown in Table IV. The simulation results of these three attacking strategies are consistent with the results according to the IC boundary removal strategy, that is, the severity of cascading failures of SED solutions is significantly lower than the power dispatch based on conventional OPF.

V. CONCLUSIONS

In this paper, the temporal weighted network that combines topological characteristics and temporal feature of operation status of power networks is proposed. In a TWN, the topological structure is static and weight distribution varies over time. Then, to intuitively quantify the risk of cascading failures, a new concept of inverse-community structure is introduced. Subsequently in the new structure, the modularity is upgraded as inverse-modularity by temporal weight to quantify the extent of IC structure. By simulation and comparison, the positive correlation between IM of power flow distribution and risk of cascading failures has been justified. Furthermore, considering the risk of cascading failures and the generation cost, the security/economic dispatch method which minimizes simultaneously two objective functions has been verified. An optimization algorithm is developed based on a genetic algorithm that treats the magnitude of two objective functions to find the Pareto-optimal solutions for the SED problem. Taking the IEEE-118 bus systems as a test case, we have proved that the proposed SED method can make proper trade-off between cascading failure risks and generation cost. To mitigate economic losses and reduce computation time, SED is only performed when IM corresponding to power flow distribution is greater than a critical value. These results demonstrate that the IC structure can provide an innovative perspective for intuitively quantifying the risk of cascading failures. IC and IM make it possible to quickly assess cascading failure risks without large-scale time-consuming post-contingency simulations. In future research, IC and IM could be promising in identifying critical components in cascading

failures and in evaluating system vulnerability in various system structures and operating states.

In this paper, we propose a removal strategy based on the power flow rank of boundaries of IC to trigger cascading failures. These boundaries may be considered as the vulnerable lines which could be targeted by intentional attacks. In the future, the relation between IC characteristic cascading failure risk could be utilized by malicious attackers. Furthermore, the IC structure would be promising to help detecting key transmission sections in power networks. Moreover, cascading failure of power system is a complex process with interaction among active power, reactive power, voltage variation and protective relaying systems. Therefore, the researches about IC will be extended to integrate with other factors for more comprehensive models in our following studies. On the other hand, cascading failures may also exist in many other engineering networks, such as transportation networks or gas pipeline networks. It would be interesting and promising to investigate if inverse-community structures also exist and are positively correlated to cascading failure risks in these networks.

REFERENCES

- [1] Y. X. Huang, J. J. Wu, W. D. Ren, C. K. Tse, and Z. B. Zheng, "Sequential Restorations of Complex Networks After Cascading Failures," *IEEE Trans. Syst. Man Cybern. -Syst.*, vol. 51, no. 1, pp. 400-411, Jan. 2021.
- [2] L. Liu, H. Wu, L. Li, D. Shen, F. Qian, and J. Liu, "Cascading Failure Pattern Identification in Power Systems Based on Sequential Pattern Mining," *IEEE Trans. Power Syst.*, vol. 36, no. 3, pp. 1856-1866, May. 2020.
- [3] J. J. Wu, Z. H. Chen, Y. H. Zhang, Y. X. Xia, and X. Chen, "Sequential Recovery of Complex Networks Suffering From Cascading Failure Blackouts," *IEEE Trans. Netw. Sci. Eng.*, vol. 7, no. 4, pp. 2997-3007, Oct 1. 2020.
- [4] W. X. Liao, S. Salinas, M. Li, P. Li, and K. A. Loparo, "Cascading Failure Attacks in the Power System: A Stochastic Game Perspective," *IEEE Internet Things J.*, vol. 4, no. 6, pp. 2247-2259, Dec. 2017.
- [5] N. N. Tran, H. R. Pota, Q. N. Tran, and J. Hu, "Designing Constraint-Based False Data-Injection Attacks Against the Unbalanced Distribution Smart Grids," *IEEE Internet Things J.*, vol. 8, no. 11, pp. 9422-9435. 2021.
- [6] Q. Yang, D. Li, W. Yu, Y. Liu, D. An, X. Yang, and J. Lin, "Toward data integrity attacks against optimal power flow in smart grid," *IEEE Internet Things J.*, vol. 4, no. 5, pp. 1726-1738. 2017.
- [7] Z. Zhang, R. Deng, D. K. Yau, and P. Chen, "Zero-Parameter-Information Data Integrity Attacks and Countermeasures in IoT-Based Smart Grid," *IEEE Internet Things J.*, vol. 8, no. 8, pp. 6608-6623. 2021.
- [8] L. D. Xing, "Cascading Failures in Internet of Things: Review and Perspectives on Reliability and Resilience," *IEEE Internet Things J.*, vol. 8, no. 1, pp. 44-64, Jan 1. 2021.
- [9] L. D. Xing, "Reliability in Internet of Things: Current Status and Future Perspectives," *IEEE Internet Things J.*, vol. 7, no. 8, pp. 6704-6721, Aug. 2020.
- [10] H. D. Guo, C. Y. Zheng, H. H. C. Iu, and T. Fernando, "A critical review of cascading failure analysis and modeling of power system," *Renew. Sust. Energ. Rev.*, vol. 80, pp. 9-22, Dec. 2017.
- [11] Z. Wang, A. Scaglione, and R. J. Thomas, "A Markov-transition model for cascading failures in power grids," in in *Proc. 45th Hawaii Int. Cond. Syst. Sci. (HICSS)*, pp. 2115-2124. 2012
- [12] J. J. Qi, "Utility Outage Data Driven Interaction Networks for Cascading Failure Analysis and Mitigation," *IEEE Trans. Power Syst.*, vol. 36, no. 2, pp. 1409-1418, Mar. 2021.
- [13] I. Dobson, B. A. Carreras, and D. E. Newman, "A loading-dependent model of probabilistic cascading failure," *Probab. Eng. Inform. Sci.*, vol. 19, no. 1, pp. 15. 2005.

- [14] Y. Koc, M. Warnier, P. Van Mieghem, R. E. Kooij, and F. M. T. Brazier, "The impact of the topology on cascading failures in a power grid model," *Physica A*, vol. 402, pp. 169-179, May 15. 2014.
- [15] P. D. H. Hines, I. Dobson, and P. Rezaei, "Cascading Power Outages Propagate Locally in an Influence Graph That is Not the Actual Grid Topology," *IEEE Trans. Power Syst.*, vol. 32, no. 2, pp. 958-967, Mar. 2017.
- [16] X. G. Wei, S. B. Gao, T. Huang, E. Bompard, R. J. Pi, and T. Wang, "Complex Network-Based Cascading Faults Graph for the Analysis of Transmission Network Vulnerability," *IEEE Trans. Ind. Inform.*, vol. 15, no. 3, pp. 1265-1276, Mar. 2019.
- [17] Z. H. Chen, J. J. Wu, Y. X. Xia, and X. Zhang, "Robustness of Interdependent Power Grids and Communication Networks: A Complex Network Perspective," *IEEE Trans. Circuits Syst. II-Express Briefs.*, vol. 65, no. 1, pp. 115-119, Jan. 2018.
- [18] V. Sarfi, and H. Livani, "An Economic-Reliability Security-Constrained Optimal Dispatch for Microgrids," *IEEE Trans. Power Syst.*, vol. 33, no. 6, pp. 6777-6786, Nov. 2018.
- [19] P. P. Biswas, P. N. Suganthan, B. Y. Qu, and G. A. J. Amarutunga, "Multiobjective economic-environmental power dispatch with stochastic wind-solar-small hydro power," *Energy*, vol. 150, pp. 1039-1057, May 1. 2018.
- [20] R. A. Jabr, A. H. Coonick, and B. J. Cory, "A homogeneous linear programming algorithm for the security constrained economic dispatch problem," *IEEE Trans. Power Syst.*, vol. 15, no. 3, pp. 930-936, Aug. 2000.
- [21] X. Lu, K. W. Chan, S. W. Xia, B. Zhou, and X. Luo, "Security-Constrained Multiperiod Economic Dispatch With Renewable Energy Utilizing Distributionally Robust Optimization," *IEEE Trans. Sustain. Energy.*, vol. 10, no. 2, pp. 768-779, Apr. 2019.
- [22] L. N. Liu, and G. H. Yang, "Distributed Optimal Economic Environmental Dispatch for Microgrids Over Time-Varying Directed Communication Graph," *IEEE Trans. Network Sci. Eng.*, vol. 8, no. 2, pp. 1913-1924, Apr-Jun. 2021.
- [23] S. Lu, W. Gu, K. Meng, and Z. Y. Dong, "Economic Dispatch of Integrated Energy Systems With Robust Thermal Comfort Management," *IEEE Trans. Sustain. Energy.*, vol. 12, no. 1, pp. 222-233, Jan. 2021.
- [24] X. Li, W. Wang, H. Wang, J. Wu, X. Fan, and Q. Xu, "Dynamic environmental economic dispatch of hybrid renewable energy systems based on tradable green certificates," *Energy*, vol. 193, pp. 116699. 2020.
- [25] S. Poudel, Z. Ni, and W. Sun, "Electrical Distance Approach for Searching Vulnerable Branches During Contingencies," *IEEE Trans. Smart Gri.*, vol. 9, no. 4, pp. 3373-3382, Jul. 2018.
- [26] M. E. J. Newman, "Analysis of weighted networks," *Phys. Rev. E.*, vol. 70, no. 5, Nov. 2004.
- [27] T. E. C. M. o. Power, "Report of the enquiry committee on grid disturbance in northern region on 30th July 2012 and in northern, eastern and north-eastern region on 31st July 2012," *Government of India.Tech. Rep.*, August. 2012.
- [28] B. Li, and G. Sansavini, "Effective multi-objective selection of inter-subnetwork power shifts to mitigate cascading failures," *Electr. Power Syst. Res.*, vol. 134, pp. 114-125, May. 2016.
- [29] P. Holme, and J. Saramaki, "Temporal networks," *Phys Rep.*, vol. 519, no. 3, pp. 97-125, Oct. 2012.
- [30] J. L. He, and D. B. Chen, "A fast algorithm for community detection in temporal network," *Physica A.*, vol. 429, pp. 87-94, Jul. 2015.
- [31] M. E. J. Newman, and M. Girvan, "Finding and evaluating community structure in networks," *Phys. Rev. E.*, vol. 69, no. 2, Feb. 2004.
- [32] M. E. J. Newman, "Modularity and community structure in networks," *Proc. Natl. Acad. Sci. U. S. A.*, vol. 103, no. 23, pp. 8577-8582, Jun 6. 2006.
- [33] C. S. Chang, D. S. Lee, L. H. Liou, S. M. Lu, and M. H. Wu, "A Probabilistic Framework for Structural Analysis and Community Detection in Directed Networks," *IEEE-ACM Trans. Netw.*, vol. 26, no. 1, pp. 31-46, Feb. 2018.
- [34] H. Jiang, Z. J. Liu, C. L. Liu, Y. S. Su, and X. Y. Zhang, "Community detection in complex networks with an ambiguous structure using central node based link prediction," *Knowl-Based Syst.*, vol. 195, May. 2020.
- [35] R. Arthur, "Modularity and projection of bipartite networks," *Physica A-Statistical Mechanics and Its Applications*, vol. 549, Jul 1. 2020.
- [36] Y. F. Zhang, Y. Y. Liu, X. M. Ma, and J. Song, "Community detection in signed networks by relaxing modularity optimization with orthogonal and nonnegative constraints," *Neural Computing & Applications*, vol. 32, no. 14, pp. 10645-10654, Jul. 2020.
- [37] D. Jin, B. B. Zhang, Y. Song, D. X. He, Z. Y. Feng, S. Z. Chen, W. H. Li, and K. Musial, "ModMRF: A modularity based Markov Random Field method for community detection," *Neurocomputing*, vol. 405, pp. 218-228, Sep 10. 2020.
- [38] S. Fortunato, "Community detection in graphs," *Physics Reports-Review Section of Physics Letters*, vol. 486, no. 3-5, pp. 75-174, Feb. 2010.
- [39] Y. Z. Li, Q. H. Wu, L. Jiang, J. B. Yang, and D. L. Xu, "Optimal Power System Dispatch With Wind Power Integrated Using Nonlinear Interval Optimization and Evidential Reasoning Approach," *IEEE Trans. Power Syst.*, vol. 31, no. 3, pp. 2246-2254, May. 2016.
- [40] Y. Koc, T. Verma, N. A. M. Araujo, and M. Warnier, "MATCASC: A tool to analyse cascading line outages in power grids," *2013 IEEE International Workshop on Intelligent Energy Systems (IWIES)*, pp. 143-148. 2013.
- [41] R. Sen Biswas, A. Pal, T. Werho, and V. Vittal, "A Graph Theoretic Approach to Power System Vulnerability Identification," *IEEE Trans. Power Syst.*, vol. 36, no. 2, pp. 923-935, Mar. 2021.
- [42] A. Beiranvand, and P. Cuffe, "A Topological Sorting Approach to Identify Coherent Cut-Sets Within Power Grids," *IEEE Trans. Power Syst.*, vol. 35, no. 1, pp. 721-730, Jan. 2020.
- [43] H. Cetinay, S. Soltan, F. A. Kuipers, G. Zussman, and P. Van Mieghem, "Comparing the Effects of Failures in Power Grids Under the AC and DC Power Flow Models," *IEEE Trans. Netw. Sci. Eng.*, vol. 5, no. 4, pp. 301-312, Oct-Dec. 2018.



Xiaoliang Wang received the Postgraduate degree in sustainable energy technology from the University of Liverpool, Liverpool, U.K., in 2018, where he is currently working toward the Ph.D. degree in electrical engineering.

His research interests include complex network and power system security.



Fei Xue was born in 1977 in Tonghua of Jilin province in China. He received the bachelor and master degrees in power system and its automation from Wuhan University, Wuhan, China, in 1999 and 2002, respectively, and the Ph.D. degree in electrical engineering from Politecnico di Torino, Torino, Italy, 2009.

He was the Deputy Chief Engineer of Beijing XJ Electric Company, Ltd and Lead Research Scientist in Siemens Eco-City Innovation Technologies (Tianjin) Company, Ltd. He is currently an Associate Professor and Head of the Department of Electrical and Electronic Engineering, Xi'an Jiaotong-Liverpool University, Suzhou, China. His research interest include power system security, virtual microgrids, electric vehicle, and transactive energy control.



Qigang Wu (Student Member, IEEE) received the B. Eng degree in Electrical Engineering from the University of Liverpool, U.K., in 2014, and the M. Eng degree in Electrical Engineering from the University of Melbourne, Australia, in 2018. He is currently working toward a Ph.D. in electrical engineering at the University of

Liverpool, U.K. His research interests include complex network theorem, energy storage system and power grid operation and planning.



Shaofeng Lu received the B.Eng. and Ph.D. degrees in electrical and electronic engineering from the University of Birmingham, Birmingham, U.K., in 2007 and 2011, respectively, and the B.Eng. degree in electrical and electronic engineering from Huazhong University of Science and Technology, Wuhan, China, in

2007.

He is currently an Associate Professor with the Shien-Ming Wu School of Intelligent Engineering (WUSIE), South China University of Technology (SCUT), Guangzhou, China. Before joining SCUT in 2019, he spent 6 years as a faculty member with Department of Electrical and Electronic Engineering, Xi'an Jiaotong-Liverpool University (XJTLU), China. His main research interests include power management strategies, railway traction system, electric vehicles, optimization techniques, and energy-efficient transportation systems.



Lin Jiang received the B.S. and M.S. degrees in electrical engineering from the Huazhong University of Science and Technology China, Wuhan, China, 1992 and 1996, and the Ph.D. degree in electrical engineering from the University of Liverpool, Liverpool, U.K. in 2001.

He is currently a Reader with the University of Liverpool. His current research interests include the optimization and control of smart grids, electrical machines, power electronics, and renewable energy.



YUE HU (Member, IEEE) was born in Yueyang, Hunan, China, in 1978. He received the B.S. and M.S. degrees from Shanghai Jiao Tong University, Shanghai, China, in 2001 and 2007, respectively, and the Ph.D. degree from the Politecnico di Torino, Turin, Italy, in 2010. In 2010, he joined the Department of Applied

Electromagnetism, Istituto Nazionale di Ricerca Metrologica, Turin, related to the characteristic of partial discharge (PD) instruments. Since 2011, he has been with Shanghai Jiao Tong University. His current research interests include the PD detection and location, and nanogrid energy systems.